PROCEEDINGS OF SCIENCE

Surface muons in IceTop

The IceCube Collaboration[1]

[1] *http://icecube.wisc.edu/collaboration/authors/icrc15_icecube*

E-mail: hdembins@udel.edu

IceTop, the surface component of the IceCube detector, has been used to measure the energy spectrum of cosmic rays over three decades from 1.6 PeV to 1.3 EeV. It was recently shown that the recorded data can also be used to measure the average density of GeV muons in the shower front at large lateral distances (> 300 m) from the shower axis. The analysis is based on fitting the single muon peak in charge histograms built over many events. The shape of this peak can be accurately modeled and stands out above the electromagnetic background at large distances. Since the analysis can be done in several lateral intervals, we effectively extract the muon lateral distribution function from data (μ-LDF). The amplitude of the μ-LDF is connected to the average cosmic-ray mass.

We will present the measurement of the μ-LDF for cosmic rays with energies between 1 PeV and 30 PeV and compare it to proton and iron simulations. By combining the μ-LDF with complementary mass-sensitive observables, like the charge deposited by muon bundles in IceCube, we expect to significantly reduce systematic uncertainties in the inferred cosmic ray mass composition due to theoretical uncertainties in hadronic interaction models.

Corresponding authors: H.P. Dembinski*, J.G. Gonzalez,
Bartol Institute, University of Delaware, USA

The 34th International Cosmic Ray Conference,
30 July- 6 August, 2015
The Hague, The Netherlands

*Speaker.

PoS(ICRC2015)267

1. Cosmic rays and muons in air showers

Cosmic rays above 0.1 PeV are detected through air showers generated in Earth's atmosphere, typically with large ground arrays of particle detectors. The origin of PeV cosmic rays is a long standing puzzle. Since cosmic rays are charged, they are bent onto complex paths by galactic and extragalactic magnetic fields [1]. The arrival direction of a cosmic ray can be accurately measured, but it does not point back to the source. The two remaining identifying properties of a cosmic ray are its energy and mass. Knowledge of the energy spectrum and mass composition of cosmic rays does help to discriminate between different origin and propagation scenarios [2], but the inference from air shower data is model-dependent, which is the main obstacle in this approach.

The model-dependence enters through air shower simulations which provide the link between the properties of the incident cosmic rays and the measurement at the ground. These simulations rely on hadronic interaction models, phenomenological interpretations of collider data, extrapolated into phase-space regions relevant for air showers. The uncertainty on how to do the extrapolation is reflected in the variety of available hadronic interaction models [2].

The best strategy under these circumstances is to collect many different experimental observables. A hadronic model can then be tested on its consistency in inferring the mass composition from these observables. If the results differ, this might point to a deficiency in the model.

If separately measured, the muon content of an air shower on the one hand, and its electron and photon content on the other, form a potent pair of variables to infer the energy E and mass A of the cosmic ray [2]. Using a Heitler-approximation of a hadronic shower [3], it has been shown that the number of electrons at shower maximum approximately scales like E, while the muon component scales like $E^{\beta}A^{1-\beta}$, with $\beta \simeq 0.9$ [4]. The energy E therefore can be deduced from the size of the electromagnetic component, and the mass A from the size of the muon component. The model-uncertainty enters through the values of β and the corresponding scaling factors, which have to be taken from simulations.

In this paper, we show a preliminary measurement of the average lateral density function of muons (μ-LDF) obtained with IceTop [5], the surface component of the IceCube Neutrino Observatory, between 1 PeV and 30 PeV. The result is an update of the analysis first presented in Ref. [6], which is a statistical study of signals collected at large lateral distances (minimum radius varies between 250 m at 1 PeV and 400 m at 100 PeV). Muon-rich signals at large lateral distances were explored before [7], but the potential to measure the muon density was realized only recently. The analysis presented here yields a high-resolution measurement due to the large exposure collected by IceTop, does not rely on detector simulation, and works over a large zenith angle range from 0° to 40° (an extension to higher angles is under study). It exploits the low trigger threshold in each detector and the fact that GeV muons have a clear signature as through-going minimum-ionizing particles in IceTop detectors.

The average density of muons at a given reference distance scales with the overall average size of the muon component. As outlined above, this implies that the measurement of μ-LDF can be converted into an estimate of the mean logarithmic mass [4]. In addition, the measurement of the μ-LDF over a large lateral range and zenith angle range provides a wealth of data, which will allow us to test the consistency of a hadronic model. The μ-LDF itself will be used in a future event-by-event fit of recorded signals [8]. Our measurement of GeV muons at the surface is complementary

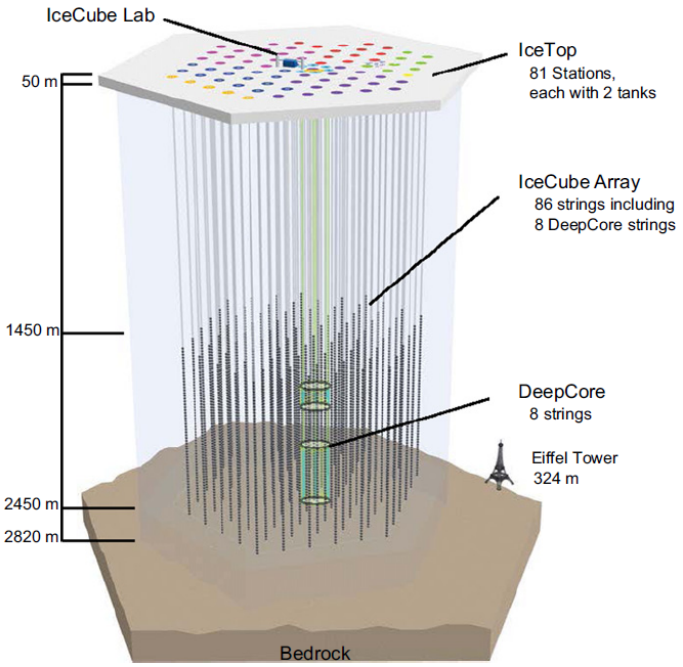

Figure 1: Schematic view of the IceCube experiment. The bulk of the light detectors are buried under 1.5 km of ice and form the in-ice detector. The in-ice detector is used mainly for neutrino astronomy and neutrino physics studies. The IceTop detector is formed by 81 pairs of ice-filled tanks at the surface. They are used to veto particles from cosmic-rays induced air showers that sometimes reach the in-ice detector, and for studies of cosmic rays at the South Pole at 2835 m altitude and an atmospheric depth of about 680 g cm^{-2}.

to ongoing analyses of muon bundles that reach IceCube [9], and the analysis of high-p_T muons accompanying these bundles [10]. A related analysis of muon-rich signals in detectors at large lateral distance is ongoing, which studies their sensitivity to the cosmic-ray mass composition [11].

2. The IceTop array

The IceTop detector is the surface component of the IceCube Neutrino Observatory, shown in Fig. 1. It consists of 81 stations on a triangular grid with mean spacing of 125 m, covering roughly one square kilometer. Each station consists of two ice-Cherenkov detectors separated by 10 m. The active volume of each detector is a cylinder with a ground area of 2.54 m^2 and a height of 0.9 m.

The detectors are sensitive to muons ($E_\mu > 0.2$ GeV), electrons and photons, but have no dedicated particle identification functionality. They measure the deposited PMT charge S, the time-integral of a localized pulse above the baseline, in units of VEM (vertical equivalent muon). The VEM is the mean charge generated by a muon passing vertically through the detector, which have a dynamic range of 0.2 to about 1000 VEM. A "Hard Local Coincidence" (HLC) occurs when two detectors from the same station trigger within a time window of 1 μs. A single local trigger without such a partner is called a "Soft Local Coincidence" (SLC).

The difference between HLCs and SLCs for our purpose is that HLC charges are better calibrated. For an HLC, the whole time trace of the pulse is recorded, which allows us to do more sophisticated off-line processing to compute the charge. For an SLC, only the total charge computed by the on-board firmware is recorded. The resolution of SLC charges used in this analysis is improved by performing an off-line cross-calibration to HLC charges. After this correction, the charge resolutions of HLCs and SLCs agree within a few percent.

Air showers are reconstructed by fitting an LDF-model to the recorded charges and a model of the curved shower front to the signal arrival times [5]. The signal S_{125} at 125 m lateral dis-

tance to the shower axis is used to quantify the size of the shower at ground, and converted into an estimate of the cosmic ray energy using simulated air showers [12]. Up to zenith angles of 40°, S_{125} is dominated by the electromagnetic component of the air shower. At large radii, $r \gtrsim 250\,(E/\mathrm{PeV})^{0.25}$ m [6], photons and electrons become less energetic and fewer in number, so that their average contribution to the signal drops below 1 VEM. At this point, the muon component may be identified.

3. Data set and analysis

We use IceTop data recorded from 1 June 2010 to 31 May 2013, processed with the standard reconstruction [12]. After standard quality cuts [12], 82 M events remain. We analyze events with zenith angles $\theta < 40°$ and shower sizes $S_{125} > 1.0$ VEM, which reduces the number to 47 M events.

The present work is an update of the analysis presented in Ref. [6]. The analysis approach was independently re-implemented from scratch, which allowed us to cross-check both implementations. The update differs from the first version in two key aspects.

Firstly, it addresses a known issue of the first implementation. Some recorded charge pulses do not originate from the air shower, but mimic muon pulses. This uncorrelated background is formed by random coincidences from other particles that hit the detector. The uncorrelated background is a significant distortion at low shower energies, where the muon density in the shower front is very small. In the first version, this contribution was subtracted based on a simple estimate of the background trigger rate, with some systematic uncertainty. In the updated version, the uncorrelated background is explicitly measured as explained below, and subtracted without uncertainty.

Secondly, the model for the expected charge distribution from pulses with muons was refined. In the first version, the distribution was tabulated from simulations of the detector response to muons. In the update, the tables were replaced by an analytical model of the detector response, whose parameters are completely determined by the data. This avoids uncertainties in the simulation of the muon response.

The analysis procedure is described in the following. For each reconstructed event, we select all recorded pulses compatible in time with the reconstructed shower front, using a window of 1.5 μs (signal window). We measure the contribution of random coincidences by selecting all pulses in an off-time window before the shower front arrives, that has a length of 8 μs (background window). Finally, we also count all detectors that were in data acquisition, whether they had a pulse in the signal window or not. Their number is needed to compute the Poisson probability for having k muon hits in a detector for a given expectation.

We then generate histograms of the charge S for the selected pulses. We generate independent histograms for bins of the lateral distance r to the shower axis, the shower size S_{125} (which is a proxy of the shower energy), and the shower zenith angle θ. Separate sets of histograms are generated for the signal and the background window, and furthermore for HLC and SLC pulses, to take their minor differences in resolution into account.

Two charge histograms are shown in Fig. 2. At large radii, we find two distinct components. The first component peaks around $S \approx 0.3$ VEM. It consists of detectors which were hit only by low-energy electrons and photons, which contribute a small fraction of a VEM per particle. The

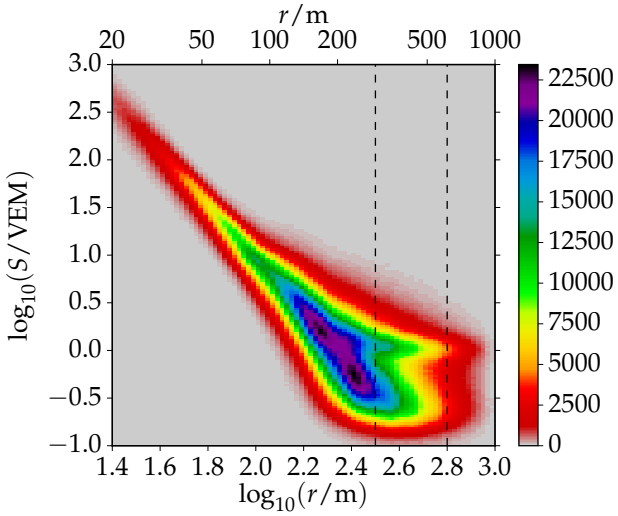

(a) 2D charge histogram (sum of HLC and SLC histograms).

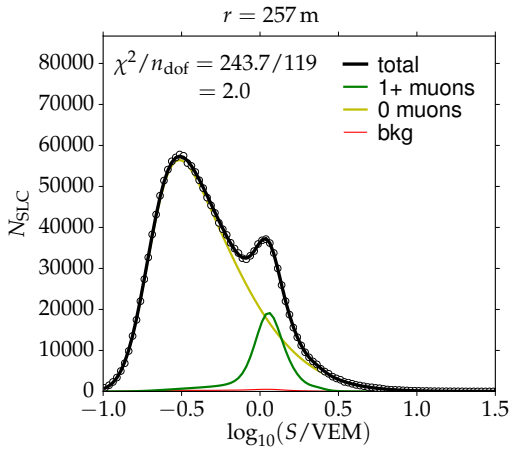

(b) Slice around $r = 257\,\mathrm{m}$.

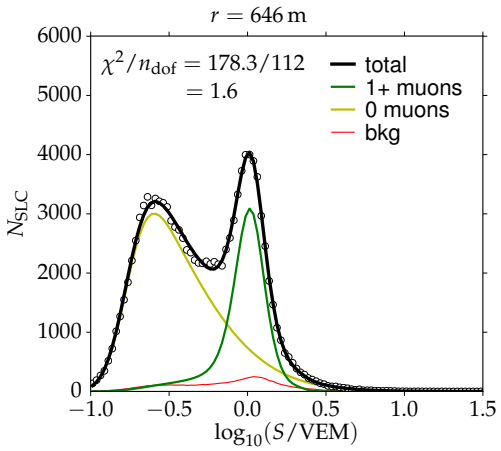

(c) Slice around $r = 646\,\mathrm{m}$.

Figure 2: Shown are histograms of recorded pulse charges S for near vertical air showers with $\langle E \rangle \approx 3\,\mathrm{PeV}$ and $\langle \theta \rangle \approx 13^\circ$. a) The dashed lines mark the slices shown in b) and c). Also shown in the slices is the model fitted to the histograms, which we use to compute the muon density per detector (thick black line), and its three components (thin lines). There is a component for hits without muons (0 muons), a component for hits with one or more muons (1+ muons), and the component for hits from uncorrelated background (bkg).

Table 1: Number of fitted parameters per charge histogram.

Model aspect	no. of parameters
signal threshold	2
shape of 0 muon-peak	2
shape of 1+ muon-peak	3
peak amplitudes	2
total	9

second component peaks around 1 VEM, and consists of detectors that were hit by at least one muon.

Our model for the charge distribution generated by muon hits is detailed and relies only on a few basic assumptions. GeV muons are distinct, because they are minimum-ionizing, penetrate the detector without being stopped, and are parallel to the shower axis within a few degrees. Particles that enter the detector through the top and leave through the base generate tracks of equal length. Since the generated Cherenkov-light is proportional to the track length and since the selected showers are close to vertical, the charges generated by muon hits are always very close to 1 VEM. This well-defined feature allows us to distinguish muon hits from other hits on a statistical basis. In principle, there is another peak for two simultaneous muons hits around 2 VEM and so on, but it is not visible in Fig. 2. These peaks are statistically suppressed, because the muon density at large lateral distances from the shower axis is very low. The chance for two simultaneous hits is very small at the radii that we consider. We model the charge distributions for up to three simultaneous muon hits and neglect higher contributions.

Mathematically, the charge distribution for hits with muons is constructed as follows. For a given muon density ρ_μ, the expected number of muon hits λ_μ per detector is computed from the effective area of the detector at the given zenith angle θ. The chance for k simultaneous muon hits is computed from the Poisson distribution with expectation λ_μ. We compute the charge distribution for $k = 1$ by folding an analytical model of the track length distribution [13] (parameter free) with an exponentially modified Gaussian kernel [14]. The kernel models the finite detector resolution and the additional charge generated by electrons and photons that accompany the muon. The approach was found to describe the simulated detector response to muons very well. The charge distribution for k simultaneous muon hits then follows from auto-convolution of the distribution for $k = 1$.

The charge distribution for pulses without muons is described empirically by the density $\sim \exp(a + b\log r + c\log^2 r)$, and no effort is made to physically interpret it. Both distributions are multiplied with a Gaussian cumulative density function in the logarithm of the signal, which models the reduced efficiency for detecting low signals, caused by the threshold trigger in each detector. This approach statistically accounts for losses of muon signals due to the threshold trigger, so that these losses are automatically corrected. In near-vertical showers, these losses are also small, since the charge in pulses with muons is usually far larger than the threshold level of 0.2 VEM.

The measured charge distribution of random coincidences (uncorrelated background) is finally added on top of these distributions. The sum of all component distributions is fitted to the data using a log-likelihood method, which then extracts the muon density ρ_μ for each lateral bin in which the muon peak is separable. The nine parameters (listed in Table 1) of our semi-analytical model are

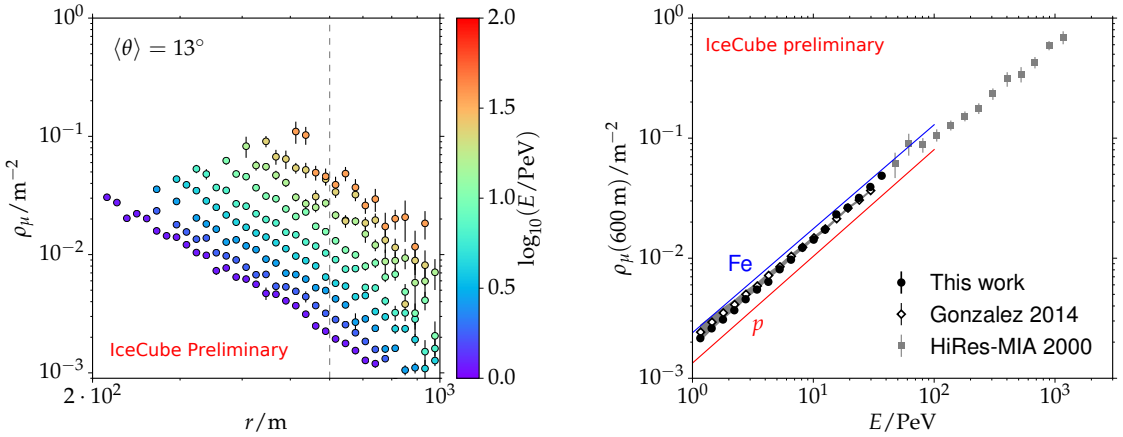

(a) Muon density as a function of radius.

(b) Muon density at 600 m radius.

Figure 3: *Left*: Average muon density ρ_μ in near-vertical showers ($\langle\theta\rangle \approx 13°$, slant depth $X \approx 700\,\mathrm{g\,cm}^2$) at various energies and lateral distances measured at the South Pole, for one month of data (June 2011). The dashed line indicates the reference radius of 600 m. *Right*: Comparison of $\rho_\mu(600\,\mathrm{m})$ obtained in this work with the corrected previous result from Gonzalez [6] (see text for details). The gray band represents the systematic uncertainty associated the approximate subtraction of uncorrelated background in the previous analysis. Shown for reference are simulation results for proton and iron showers, generated with CORSIKA, using Sibyll-2.1 and Fluka [15, 16, 17]. Also shown for reference is a measurement from HIRES-Mia in Utah, Colorado [18]. The latter is located at a different slant depth of $X \approx 860\,\mathrm{g\,cm}^{-2}$.

completely determined by data, and fitted independently to each charge histogram.

The effective energy threshold for our method is given by the energy required for muons to fully penetrate the ice volume inside a detector and the snow layer on top of it. The latter varies between 0.1 m and 3 m. The density of snow at the South Pole is about $0.4\,\mathrm{g\,cm}^{-3}$ [5], so that we obtain an effective energy threshold of $\left(0.16 + 0.08\,h_{\mathrm{snow}}[\mathrm{m}]\right)\,\mathrm{GeV}/\cos\theta$ due to ionization losses, where h_{snow} is the snow height in meter. The muons that we investigate have typical energies of a few GeV, therefore we do not expect significant losses in near-vertical showers. We will experimentally investigate the impact of the snow layer by comparing detectors in different depths in the future.

4. Preliminary results and outlook

In Fig. 3, we show our preliminary estimate of the average muon density ρ_μ in near-vertical air showers between 1 PeV and 30 PeV from one month of data (June 2011). Overlaid are estimates of $\rho_\mu(600\,\mathrm{m})$ from the first presentation of the analysis [6], which have been modified here to correct a calculation error that was discovered after comparing the two analysis implementations. The error had made our initial estimate of $\rho_\mu(600\,\mathrm{m})$ by a factor of about 1.5 too high. Both results are in very good agreement after the correction.

The HiRes-MIA and the Pierre Auger collaborations reported muon densities above 50 PeV and 5 EeV respectively [18, 4] which exceeded expectations from all tested hadronic interaction

models. In Fig. 3, we compared our estimate with CORSIKA simulations for proton and iron showers using the hadronic interaction models Sibyll-2.1 and Fluka [15, 16, 17]. The simulations bracket our data. We will follow up on this investigation by comparing to more hadronic interaction models, once our results are final.

The next step towards finalizing the analysis is to perform a check of our approach based on an analysis of fully detector-simulated air showers. We want to determine how well our fits of charge histograms estimate the true muon density in CORSIKA showers, computed from the muon hits at the ground. We will also investigate the effect of snow on top of detectors and possible variations of the measured muon density over time.

A future publication of our results will contain the μ-LDF measured over a wider range of shower energies and zenith angles, together with suitable parametrizations of the data. This will allow us to make several interpretations: The muon density ρ_μ at 600 m scales with the size of the muon component of an air shower, while the standard energy proxy of IceTop, the signal S_{125} at 125 m scales primarily with the electromagnetic component. Following the analysis outlined in the introduction, and recently applied in Ref. [4], we will transform these two measurements into an estimate of the mean logarithmic mass $\langle \ln A \rangle$ of cosmic rays using Sibyll-2.1 and more recent hadronic interaction models. In addition, we will investigate the muon attenuation with zenith angle. The muon attenuation is also sensitive to the mass composition and allows us to test the internal consistency of a hadronic interaction model, since it has to predict both the size and the attenuation of the muon component in agreement with our data.

References

[1] R. Jansson and G.R. Farrar, *Astrophys. J.* **757** (2012) 14.

[2] K.-H. Kampert, M. Unger, *Astropart. Phys.* **35** (2012) 660.

[3] J. Matthews, *Astropart. Phys.* **22** (2005) 387.

[4] **Pierre Auger** Collaboration, A. Aab et al., *Phys. Rev. D* **91** (2015) 032003.

[5] **IceCube** Collaboration, R. Abbasi et al., *Nucl. Instrum. Meth. A* **700** (2013) 188.

[6] **IceCube** Collaboration, J.G. Gonzalez et al., *Measuring the Muon Content of Air Showers with IceTop*, in *Proc. ISVHECRI 2014*, CERN, Switzerland (2014), [arXiv:1501.03415].

[7] M. Vraeghe, Master thesis: *Muon Counting with the IceTop Detector as Probe of Cosmic Ray Composition*, Gent University, Belgium (2012).

[8] **IceCube** Collaboration, J.G. Gonzalez et al., PoS(ICRC2015)338 *these proceedings* (2015).

[9] **IceCube** Collaboration, K. Rawlins et al., PoS(ICRC2015)628 *these proceedings* (2015).

[10] **IceCube** Collaboration, D. Soldin et al., PoS(ICRC2015)256 *these proceedings* (2015).

[11] D. Bindig, PhD thesis in preparation: *Measuring muons in IceTop*, Wuppertal University, Germany (2015).

[12] **IceCube** Collaboration, M.G. Aartsen et al., *Phys.Rev. D* **88** (2013) 042004.

[13] B. Kégl and D. Veberič, *Pierre Auger Observatory note GAP-2009-043* (2009), [arXiv:1502.03347].

[14] E. Grushka, *Analytical Chemistry* **44** (1972) 1733.

[15] D. Heck, G. Schatz, T. Thouw, J. Knapp, and J. N. Capdevielle, *Report No. FZKA 6019* (1998).

[16] R.S. Fletcher, T.K. Gaisser, P. Lipari, T. Stanev, *Phys. Rev. D* **50** (1994) 5710; in *Proc. 26th Int. Cosm. Ray Conf., vol. 1*, Salt Lake City, USA (1999) 415.

[17] A. Ferrari, P.R. Sala, A. Fassò, and J. Ranft, *CERN-2005-10* (2005), *INFN/TC_05/11, SLAC-R-773*.

[18] **HiRes-MIA** Collaboration, T. Abu-Zayyad et al., *Phys. Rev. Lett.* **84** (2000) 4276.